Reflection asymmetry in ^{220}Th and dinuclear model

T.M. Shneidman*, G.G. Adamian*, N.V. Antonenko*, R.V. Jolos* and W. Scheid†

*Joint Institute for Nuclear Research, 141980 Dubna, Russia
†Institut für Theoretische Physik der Justus-Liebig-Universität, D–35392 Giessen, Germany

Abstract. The negative parity bands with different values of K in ^{220}Th are analyzed within the dinuclear system model which was previously used for description of the ground state alternating-parity bands with $K = 0$ in deformed actinides. The model is based on the assumption that the cluster type shapes are produced by the collective motion in the mass-asymmetry coordinate. To describe the reflection-asymmetric collective modes characterized by the nonzero values of K, the intrinsic excitations of clusters are taken into account. The observed excitation spectrum, angular momentum dependence of the parity splitting and of the staggering behavior of the $B(E1)/B(E2)$ ratios are explained.

Keywords: dinuclear system
PACS: 21.60.Ev,21.60.Gx

INTRODUCTION

In the even-even isotopes of actinides and also in the heavy Ba and Ce isotopes the low-lying negative parity states are observed together with the usually presented collective positive-parity states combined into rotational or quasirotational ground-state bands. Formation of the positive-parity rotational or quasirotational bands is connected in general to the quadrupole collective motion, while the lowering of the negative-parity states is a signature of the presence of the reflection asymmetric collective mode. There are several approaches to treat the collective motion related to the reflection asymmetric degrees of freedom. One of them is based on the concept of the nuclear mean field [1] which has a static mirror asymmetric deformation or is characterized by a large amplitude of reflection asymmetric vibrations around the equilibrium shape. Another approach is based on the assumption that the reflection asymmetric shape is a consequence of the α-clustering in nuclei [2]. It is also known from the Nilsson-Strutinsky type calculations for light nuclei that nuclear configurations corresponding to the minima of the potential energy contain particular symmetries which are related to certain cluster structures [3, 4]. Several calculations performed for heavy nuclei [5, 6, 7] have shown that configurations with large equilibrium quadrupole deformations and low-lying collective negative parity states are strongly related to clustering. We mention also a different approach to description of the properties of the alternating parity bands which is based on the idea of the aligned octupole phonons [8, 9].

The main idea of the cluster model developed in [7, 10, 11] is that a dynamics of a reflection asymmetric collective motion can be treated as a collective motion of nucleons

between two clusters or as a motion in a mass-asymmetry coordinate. Such collective motion simultaneously creates deformations with even and odd-multipolarities. The choice of the collective coordinates and the procedure of the calculation of the potential energy and of the inertia coefficients for the Hamiltonian of the model are based on the concept of the dinuclear system (DNS). This concept was first introduced to explain the experimental data on deep inelastic and fusion reactions. Later on it was applied to the description of the nuclear structure phenomena, like alternating parity bands, mentioned above, and superdeformed states [12, 13]. The dinuclear system (A,Z) consists of two fragments (A_1,Z_1) and (A_2,Z_2) with $A = A_1 + A_2$ and $Z = Z_1 + Z_2$ kept in touching configuration by a a molecular-type nucleus-nucleus potential. As it was shown by our calculations, the α-cluster DNS ${}^{A}Z \rightarrow^{(A-4)} (Z-2)+{}^{4}$He gives a significant contribution to the formation of the low-lying nuclear states. This is also in agreement with the fact that these nuclei are good alpha-emitters.

Within this approach the existing experimental data on the angular momentum dependence of the parity splitting in the excitation spectra and the multipole transition moments (E1,E2,E3) of the low-lying alternating parity states in odd and even actinides ${}^{220-228}$Ra, ^{223,225,227}Ac, ${}^{222-224,226,228-232}$Th, ^{231}Pa, ${}^{232-234,236,238}$U and ^{240,242}Po and the medium mass nuclei ^{144,146,148}Ba, ^{151,153}Pm, ^{146,148}Ce ^{153,155}Eu and ^{146,148}Nd are well described. The good agreement between the results of calculations and the experimental data support a cluster interpretation of the reflection-asymmetric states.

However, previously we have considered in the even-even nuclei only the low-lying collective negative parity states with K=0. At the same time, there are experimental data which indicate on a presence of the low-lying collective states related to the reflection-asymmetric modes which are characterized by nonzero values of K. It can happens also that K is not a good quantum number if nuclei are located in a transitional region between deformed and spherical ones. A good example is ^{220}Th [14] whose energy spectra is a challenge for the theoretical approaches. To describe in the framework of the cluster approach the properties of the low-lying collective states related to the reflection-asymmetric collective mode and characterized by nonzero values of K we should take into account intrinsic excitations of the clusters forming a nucleus under consideration. It is the aim of the present investigation to extend the dinuclear system model to take into account such excitations.

MODEL

Hamiltonian

As illustrated in Fig. 1, the degrees of freedom chosen to characterize a dinuclear system with nearly spherical heavy cluster are related to description of the rotation of the DNS as a whole, the quadrupole oscillations of the heavy fragment, and the transfer of nucleons between the fragments. The Hamiltonian of the model can be presented in the form

$$\hat{H} = \hat{H}_0 + \hat{V}_{int}, \tag{1}$$

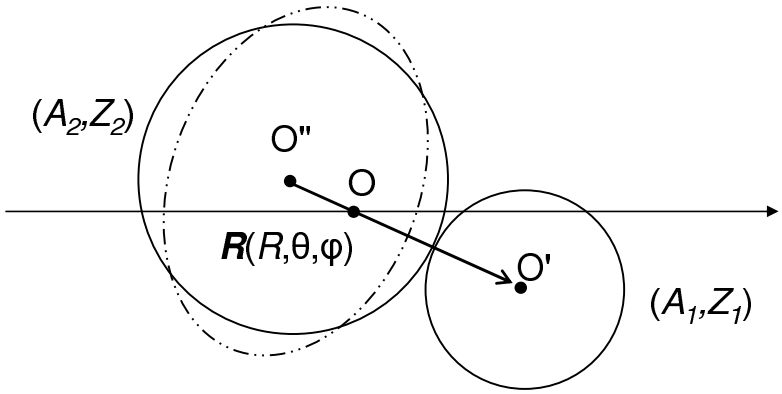

FIGURE 1. Schematic picture illustrates degrees of freedom used in the model to describe dinuclear system. Orientation of the vector of the relative distance R is defined by the angles $\Omega(\theta,\phi)$ with respect to the laboratory frame system.

where $\hat{H}_0$ describes independent fragments of the system and $\hat{V}_{int}$ describes the interaction between the fragments.

We assume that the heavy cluster is spherical and perform harmonic quadrupole oscillations around the spherically symmetric shape with frequency $\hbar\omega_0$, while the light cluster stays in its ground state. This assumption is in agreement with the suggestion made in [19] that some nuclei in the region of N=130 may have a shape with a significant octupole deformation but a negligible quadrupole deformation.

Then for $\hat{H}$ we have the following expression

$$\hat{H} = \hbar\omega_0\hat{n} + \frac{\hbar^2}{2\mu(\xi)R^2}\hat{L}^2 - \frac{\hbar^2}{2B_\xi}\frac{1}{\xi}\frac{\partial}{\partial\xi}\xi\frac{\partial}{\partial\xi} + U(R,\xi,\alpha_{2\mu}), \tag{2}$$

where, for convenience, we use positively-defined variable ξ instead of a usual definition of the mass-asymmetry coordinate $\eta = (A_1 - A_2)/(A_1 + A_2)$

$$\xi = 2A_2/A = 1 - \eta. \tag{3}$$

In equation (2), $\mu(\xi)$ is the reduced mass of the DNS, $R(\xi)$ is the distance between the centers of mass of the fragments, $\hat{n}$ is the operator of the number of the quadrupole phonons of heavy cluster, $\alpha_{2\mu}$ describes quadrupole oscillations of the surface of the heavy fragment and $\hat{L}^2$ is the operator of the square of angular momentum of the relative rotations of the two fragments

$$L^2 = -\left[\frac{1}{\sin\theta}\frac{\partial}{\partial\theta}\sin\theta\frac{\partial}{\partial\theta} + \frac{1}{\sin^2\theta}\frac{\partial^2}{\partial\phi^2}\right]. \tag{4}$$

Angles $\Omega = (\theta,\phi)$ (see Fig.1) describes the orientation of the relative distance vector $\mathbf{R}$ with respect to the laboratory coordinate system.

Above, B_ξ is a mass tensor and $U(R,\xi,\alpha_{2\mu})$ is a potential energy. The potential energy of the dinuclear system is determined as

$$U(R,\xi,\alpha_{2\mu}) = B_1 + B_2 - B_{12} + V(R,\xi,\alpha_{2\mu}). \tag{5}$$

Here, B_1, B_2 and B_{12} are the binding energies of the fragments and the compound nucleus, respectively. The nucleus-nucleus potential in (5)

$$V(R,\xi,\alpha_{2\mu}) = V_{Coul}(R,\xi,\alpha_{2\mu}) + V_{nucl}(R,\xi,\alpha_{2\mu}) \tag{6}$$

is the sum of the Coulomb potential

$$V_{Coul}(R,\xi,\alpha_{2\mu}) = \frac{e^2 Z_1 Z2}{R} + \frac{3}{5}\frac{e^2 Z_1 Z2}{R^3} R_{01}^2 \sum_{\mu} \alpha_{2\mu}^* Y_{2\mu}(\theta,\phi) + ... \tag{7}$$

and the nuclear interaction potential

$$V_{nucl}(R,\xi,\alpha_{2\mu}) = \int \rho_1(\mathbf{r_1})\rho_1(\mathbf{R}-\mathbf{r_2})F(\mathbf{r_1}-\mathbf{r_2})d^3\mathbf{r_1}d^3\mathbf{r_2}, \tag{8}$$

where $F(\mathbf{r_1}-\mathbf{r_2})$ is a Skyrme-type density dependent effective nucleon-nucleon interaction. V_{nucl} can be expanded in degrees of $\alpha_{2\mu}$. The procedure of calculation used in this paper is described in [17]. Since in our case the amplitude of the quadrupole oscillations is small only the terms linear in $\alpha_{2\mu}$ in the expansion of $V(R,\xi,\alpha_{2\mu})$ are considered. Thus, $V(R,\xi,\alpha_{2\mu})$ can be presented as

$$V(R,\xi,\alpha_{2\mu}) = V(R,\xi) + V_0(\xi)\sum_{\mu} \alpha_{2\mu}^* Y_{2\mu}(\theta,\phi), \tag{9}$$

where V_0 is determined by the nuclear and Coulomb parts of the nucleus-nucleus interaction potential. For the H_0 and V_{int} we obtain

$$\hat{H}_0 = \hbar\omega_0\hat{n} + \frac{\hbar^2}{2\mu(\xi)R^2}\hat{L}^2 - \frac{\hbar^2}{2B_\xi}\frac{1}{\xi}\frac{\partial}{\partial\xi}\xi\frac{\partial}{\partial\xi} + V(R,\xi), \tag{10}$$

and

$$V_{int} = V_0(\xi)\sum_{\mu} \alpha_{2\mu}^* Y_{2\mu}(\theta,\phi). \tag{11}$$

In this paper $\hbar\omega_0$ is considered as a free parameter which is fixed by the description of the energy of 2_1^+ state. The numerical calculation have shown that E(2_1^+) is described if we take $\hbar\omega_0$=0.47 MeV. Below we assume that the value of R is fixed and corresponds to the touching configuration of two clusters forming a dinuclear system with mass asymmetry ξ. Thus, $R = R(\xi)$.

Our analysis of the mass-asymmetry motion in ^{220}Th have shown that the motion in coordinate ξ can be separated from the other degrees of freedom and the system is in its lowest state with respect to the mass-asymmetry. The reason for this is that the energy of the first exited state related to the mass-asymmetry degree of freedom is high enough to neglect its influence on the low-energy part of the spectra. Neglecting the excitations in the variable ξ we average Hamiltonian $\hat{H}$ over $\Psi_0(\xi)$ which describes motion in ξ in the ground-state. As a result we obtain

$$\hat{H}_0 = \hbar\omega_0\hat{n} + \frac{\hbar^2}{2\mu(\xi_0)R(\xi_0)^2}\hat{L}^2 + E_0(\xi_0). \tag{12}$$

Averaging over $\Psi_0(\xi)$, yield the effective value of ξ, namely, ξ_0 located between ξ=0, which corresponds to the mononucleus configuration and $\xi = \xi_\alpha = 8/A$. In equation (12) $E_0(\xi_0)$ is the zero-point energy of the motion in ξ, which is unimportant for further consideration. The calculation have been performed with ξ_0=0.2ξ_α. Using this value of ξ_0 we can calculate the interaction energy of the dinuclear system as described in [17]. This gives $V_0(\xi_0)$=11 MeV for the interaction between vibrational and rotational degrees of freedom (see Eq.(11)).

The collective quadrupole coordinate $\alpha_{2\mu}$ can be expressed in terms of the creation and annihilation operators of the quadrupole bosons

$$\hat{\alpha}_{2\mu} = \beta_0(d^+_{2\mu} + \tilde{d}_{2\mu}), \tag{13}$$

with $\beta_0 = \sqrt{\hbar/2B\omega_0}$. Again, as in the case of $\hbar\omega_0$, the mass parameter of the quadrupole motion B is not fixed in the model. The value of B and, respectively, β_0 can be retrieved by fitting the experimental value $B(E2, 2^+ \to 0^+)$. According, to [18], the reduced transition probabilities for the lowest levels of ^{220}Th satisfy the rotor model expression with quadrupole model Q_0=540 e fm^2. This yields β_0=0.12.

If we neglect the interaction term $\hat{V}_{int}$ in (1) the eigenfunctions of the Hamiltonian can be constructed as

$$\Psi^{IM}_{(n\tau n_\Delta I_1)I_2} = [|n\tau n_\Delta I_1) \times Y_{I_2}]_{(IM)}\,, \tag{14}$$

where $|n\tau n_\Delta I_1)$ represents the n-boson wave function of the heavy nucleus, with the seniority τ and angular momentum I_1. Since the quadrupole oscillations have positive parity, the parity of the states (14) is determined by the angular momentum of the relative rotation of the fragments $p = (-1)^{I_2}$. The energies of the states (14) are given in this approximation by the expresssion

$$E_{nI_1I_2I} = \left[\hbar\omega_0 n + \frac{\hbar^2}{2\mu R^2} I_2(I_2+1)\right]. \tag{15}$$

The set of the wave functions (14) can be used as a basis to construct the eigenfunction of the Hamiltonian $\hat{H}$ in the form

$$\Psi_{IM,p} = \sum_{I_1 I_2} \sum_{n_{I_1}\tau_{I_1}} a^{(I,p)}_{n_{I_1}\tau_{I_1}I_1I_2} [|n_{I_1}\tau_{I_1}I_1) \times Y_{I_2}]_{(IM)}\,, \tag{16}$$

where coefficients $a^{(I,p)}_{n_{I_1}\tau_{I_1}I_1I_2}$ should be obtained by a diagonalization of $\hat{H}$. The matrix elements of $\hat{V}_{int}$ between the states (14) have the following form

$$\begin{aligned}\langle \Psi^{IM}_{(n'\tau'I'_1)I'_2} | \hat{V}_{int} | \Psi^{IM}_{(n\tau I_1)I_2} \rangle \quad &= (-1)^{I_1+I'_2+I} V_0\beta_0 \sqrt{\frac{5}{4\pi}(2I_2+1)}(I_2020|I'_20) \\ &\times \begin{pmatrix} I'_2 & I'_1 & I \\ I_1 & I_2 & 2 \end{pmatrix} (n'\tau'I'_1||(d^+ + \tilde{d})||n\tau I_1),\end{aligned} \tag{17}$$

where the reduced matrix elements of the boson operators can be calculated using the boson fractional parentage coefficients

$$\left[d^{n-1}(\alpha_1 I_1)dI|\}d^n\alpha I\right] = \frac{1}{\sqrt{n}}\frac{1}{\sqrt{2I+1}}(d^n\alpha I||d^+||d^{n-1}\alpha_1 I_1)$$
$$\left[d^{n-1}(\alpha_1 I_1)dI|\}d^n\alpha I\right] = (-1)^{I-I_1}\frac{1}{\sqrt{n}}\frac{1}{\sqrt{2I+1}}(d^{n-1}\alpha_1 I_1||\tilde{d}||d^n\alpha I). \quad (18)$$

Two-level solution

Although our calculations have been performed using a sufficiently large basis providing convergence the calculations have shown that the ground-state band and the first excited negative parity band can be presented with a good accuracy as a superposition of two basis states of the form (14). For the ground state band the two level approximation yields the wave function of the form (I can have only even values)

$$\Psi_I^{g.s.} = \sin[\gamma_0(I)]\left[|\frac{I}{2}\frac{I}{2}I)\times Y_0\right]_{(IM)} - \cos[\gamma_0(I)]\left[|\frac{I-2}{2}\frac{I-2}{2}(I-2))\times Y_2\right]_{(IM)} \quad (19)$$

where

$$\sin[\gamma_0(I)] = \frac{1}{\sqrt{2}}\left(1+\frac{1}{\sqrt{1+\left(\frac{V_0\beta_0}{\sqrt{2\pi}\Delta}\right)^2 I}}\right)^{1/2} \quad (20)$$

and for the energy we obtain

$$\varepsilon_I^{g.s.} = \hbar\omega\frac{I}{2} + \frac{\Delta}{2}\left[1-\sqrt{1+\left(\frac{V_0\beta_0}{\sqrt{2\pi}\Delta}\right)^2 I}\right]. \quad (21)$$

In the last expressions $\Delta = \frac{3\hbar^2}{\mu R^2} - \hbar\omega$.

For the first excited negative parity band we have

$$\Psi_I^{n.p.} = \sin[\gamma_1(I)]\left[|\frac{I-1}{2}\frac{I-1}{2}(I-1))\times Y_1\right]_{(IM)} + \cos[\gamma_1(I)]\left[|\frac{I+1}{2}\frac{I+1}{2}(I+1))\times Y_1\right]_{(IM)}, \quad (22)$$

where

$$\sin[\gamma_1(I)] = \frac{1}{\sqrt{2}} \left(1 + \frac{1}{\sqrt{1 + \left(\sqrt{\frac{12}{5\pi}} \frac{V_0 \beta_0}{\hbar\omega} \right)^2 \frac{(I+1)(2I+3)}{(2I+1)}}} \right)^{1/2} \tag{23}$$

and the energy is given as

$$\varepsilon_I^{n.p.} = \hbar\omega \frac{(I-1)}{2} + \frac{\hbar^2}{\Im} + \hbar\omega \left[1 - \sqrt{1 + \left(\sqrt{\frac{12}{5\pi}} \frac{V_0 \beta_0}{\hbar\omega} \right)^2 \frac{(I+1)(2I+3)}{(2I+1)}} \right]. \tag{24}$$

Angular momentum I can take only odd values.

Multipole Moments

Electric multipole operators are given by the expression

$$\hat{Q}_{\lambda\mu} = \int \rho(\mathbf{r}) r^\lambda Y^*_{\lambda\mu} d\tau. \tag{25}$$

For the dinuclear system we assume that

$$\rho(\mathbf{r}) = \rho_1(\mathbf{r}) + \rho_2(\mathbf{r}), \tag{26}$$

where ρ_i $(i = 1,2)$ are the densities of the DNS fragments. Using (26) we can rewrite the expression of the electric multipole moments for the DNS in the following form

$$\hat{Q}_{\lambda\mu} = \sum_{\lambda_1, \lambda_1+\lambda_2=\lambda} \sqrt{\frac{4\pi(2\lambda+1)!}{(2\lambda_1+1)!(2\lambda_2+1)!}} \left[\hat{q}_{\lambda_1}^{(\lambda_1\lambda_2)} \times Y_{\lambda_2}(\Omega) \right]_{\lambda\mu}, \tag{27}$$

where

$$\hat{q}_{\lambda_1}^{(\lambda_1\lambda_2)} = \left[\left(\frac{A_1}{A} \right)^{\lambda_2} Q_{\lambda_1}^{(2)} + (-1)^{\lambda_2} \left(\frac{A_2}{A} \right)^{\lambda_2} Q_{\lambda_1}^{(1)} \right] R^{\lambda_2}. \tag{28}$$

In the last expression $Q^{(i)}$ $(i = 1,2)$ are the intrinsic multipole moments of the DNS fragments.

Since we assume that the light fragment is spherical and can not be excited in the considered energy range the only nonzero moment for the first fragment is $Q_0^{(1)} = Z_1/\sqrt{4\pi}$. The second fragment is assumed to perform the quadrupole oscillations around

the spherical shape. Thus, in the linear approximation with respect to the deformation, we have two nonzero moments for the second fragment: $Q_0^{(2)} = Z_2/\sqrt{4\pi}$ and $Q_2^{(2)} = \frac{3Z_2R_2^2}{4\pi}\alpha_{2\mu}^*$. Therefore, we can write the explicit expressions for the dipole and quadrupole moment of the DNS in the form

$$Q_{1\mu} = e\frac{A_1Z_2 - A_2Z_1}{A}R \cdot Y_{1\mu}(\Omega) \tag{29}$$

for the dipole moment and

$$Q_{2\mu} = e\frac{A_1^2Z_2 + A_2^2Z_1}{A^2}R^2 \cdot Y_{2\mu}(\Omega) + Q_{(2)}^{2\mu} \tag{30}$$

for the quadrupole moment.

Reduced transition probabilities

Using expression (16) for the wave function and (27) for the multipole operators we can calculate the reduced transition probabilities as the

$$B(E\lambda, I_i \to I_f) = \frac{|<I_f||Q_\lambda||I_i>|^2}{2I_i+1} \tag{31}$$

The reduced matrix elements for the multipole operator Q_λ between the initial state i and the final state j has the following form

$$\begin{aligned}
&<I_jp_j||Q_\lambda||I_ip_i>= \\
&\sum_{\lambda_1\lambda_2}\sum_{\{i\}\{j\}} a_{n_{I_1}\tau_{I_1}I_1I_2}^{(I_jp_j)*} a_{n_{I_1'}\tau_{I_1'}I_1'I_2'}^{(I_ip_i)} (n_{I_1}\tau_{I_1}I_1||q_{\lambda_1}^{(\lambda_1\lambda_2)}||n_{I_1'}\tau_{I_1'}I_1')C_{I_2'0\lambda_20}^{I_20}\sqrt{\frac{(2\lambda+1)!}{(2\lambda_1+1)!(2\lambda_2+1)!}} \\
&\times\sqrt{(2i+1)(2j+1)(2\lambda+1)(2i_2+1)(2\lambda_2+1)}\begin{Bmatrix} I_1 & I_2 & I_j \\ I_1' & I_2' & I_i \\ \lambda_1 & \lambda_2 & \lambda \end{Bmatrix},
\end{aligned} \tag{32}$$

where $\lambda_1 = \lambda - \lambda_2$, and $\{i\}(\{j\})$ stands for the set of quantum numbers of the initial (final) states.

Using the two-level solutions for the ground-state and the first excited negative parity bands we can easily calculate the $B(E2)$-values for the intraband transitions and the values of $B(E1)$ for the transitions between these bands.

In the case of the quadrupole transitions we have for the transitions between the states of the ground state band

$$\begin{aligned}
&B(E2, I^{g.s.} \to (I-2)^{g.s.}) = \\
&(-q_0^{(2,0)}\sin[\gamma_0(I)]\cos[\gamma_0(I-2)] + q_2^{(0,2)}\sqrt{\frac{I}{2}}\sin[\gamma_0(I)]\sin[\gamma_0(I-2)] \\
&+q_2^{(0,2)}\sqrt{\frac{(I-2)}{2}}\cos[\gamma_0(I)]\cos[\gamma_0(I-2)])^2
\end{aligned} \tag{33}$$

and for the transition between the negative parity states

$$B(E2, I^{n.p.} \to (I-2)^{n.p.}) =$$
$$(-q_0^{(2,0)} \sqrt{\frac{6(2I-3)}{5(2I-1)}} \sin[\gamma_0(I)] \cos[\gamma_0(I-2)] + q_2^{(0,2)} \sqrt{\frac{I-1}{2}} \sin[\gamma_0(I)] \sin[\gamma_0(I-2)]$$
$$+ q_2^{(0,2)} \sqrt{\frac{(2I-3)(2I+3)(I+1)}{2(2I-1)(2I+1)}} \cos[\gamma_0(I)] \cos[\gamma_0(I-2)])^2. \quad (34)$$

In the last two expressions we have

$$q_0^{(2,0)} = e_{eff} \frac{A_1^2 Z_2 + A_2^2 Z_1}{A^2} R^2,$$
$$q_2^{(0,2)} = e_{eff} \frac{3}{4\pi} Z_1 R_1^2 \beta_0. \quad (35)$$

For the dipole transitions between the two bands our calculations yields

$$B(E1, I^{g.s.} \to (I-1)^{n.p.}) =$$
$$\frac{q_0^2}{2I+1} \left\{ \sqrt{2I-1} \sin[\gamma_0(I)] \cos[\gamma_1(I-1)] + \sqrt{\frac{6(2I+1)}{5}} \cos[\gamma_0(L)] \sin[\gamma_1(I-1)] \right\}^2,$$
$$B(E1, I^{n.p.} \to (I-1)^{g.s.}) = q_0^2 \sin^2[\gamma_1(I)] \sin^2[\gamma_0(I-1)], \quad (36)$$

where

$$q_0 = e_{eff} \frac{A_1 Z_2 - A_2 Z_1}{A} R.$$

RESULTS OF CALCULATIONS

The results of calculations of the energy spectra of the ground state band and the two lowest negative parity bands for the ^{220}Th are presented in Fig.2 together with the available experimental data. the The Hamiltonian (1) has been diagonalized numerically. One can see the overall good agreement between the calculated and experimental spectra.As a consequence of the harmonic quadrupole oscillations of the heavy fragment, the ground-state band and the first negative parity bands exhibit approximately an equidistant spectra.

The calculation shows that mainly two eigenvectors of $\hat{H}_0$ are present in the wave function of the states of the ground state band. Namely, $\left[|\frac{I}{2}\frac{I}{2}(I)) \times Y_0\right]_{(IM)}$ and $\left[|\frac{I-2}{2}\frac{I-2}{2}(I-2)) \times Y_2\right]_{(IM)}$. The contribution of the first of them is predominant at low angular momenta. As a consequence at low angular momenta the ground state band has an equidistant spectrum with the energy differences determined mainly by the frequency of the harmonic quadrupole oscillations of the heavy fragment. With increase of the angular momentum, the distance between the levels is slightly increased, due to the growing admixture of the component $\left[|\frac{I-2}{2}\frac{I-2}{2}(I-2)) \times Y_2\right]_{(IM)}$ to the wave function.

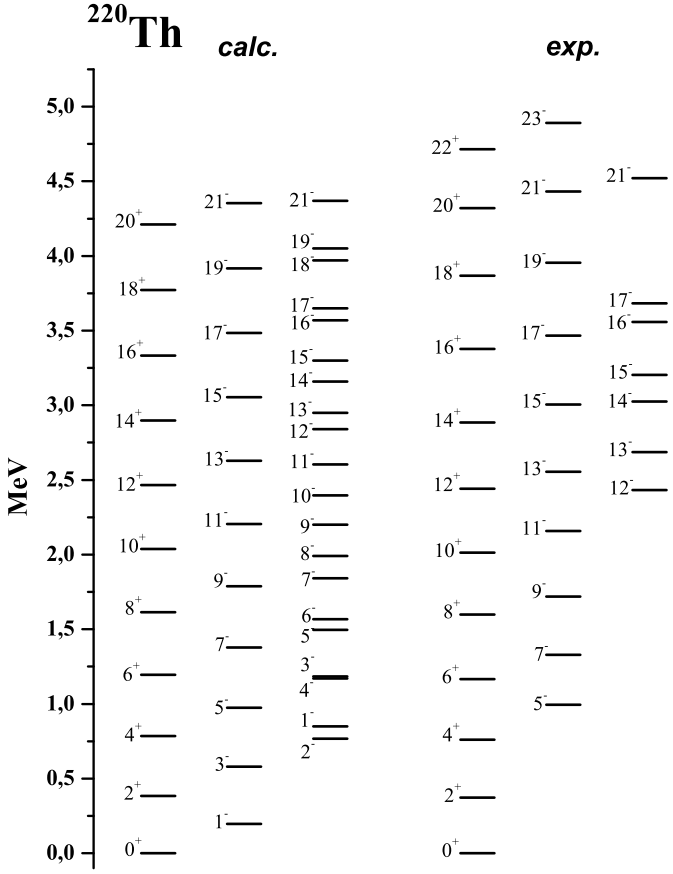

FIGURE 2. Calculated and experimental level scheme of ^{220}Th. Experimental energies, spin and parity assignments are taken from [14].

This introduces a small nonlinear dependence of the γ-transition energies on the angular momentum.

The same equidistant structure with the frequency slightly growing with angular momentum holds for the first negative parity band. Again, the calculation shows that mainly two eigenstates of $\hat{H}_0$ are present in the wave function. Namely, $\left[|\frac{I-1}{2}\frac{I-1}{2}(I-1))\times Y_1\right]_{(IM)}$ and $\left[|\frac{I+1}{2}\frac{I+1}{2}(I+1))\times Y_1\right]_{(IM)}$. The contribution of the later component while being small at I=0 is growing with angular momentum. The energy differences between the states in the negative parity band at low angular momentum are again determined mainly by the frequency of the quadrupole oscillations of the heavy fragment.

The angular momentum dependence of the frequency $\omega_{vib} = E_\gamma/2$, defined as a half of the energy difference between the energies of two neighborhood levels of the ground state band and of the first excited negative parity band is illustrated in Fig.3. One can see the sharp decrease of the experimental values of E_γ for the transition $10^+ \to 8^+$ in the ground state band and for the transition $13^- \to 11^-$ in the negative parity band which can be a consequence of the backbending phenomena. The backbending in these bands can be related to a rotational alignment of the nucleonic orbitals as it is mentioned in [14].

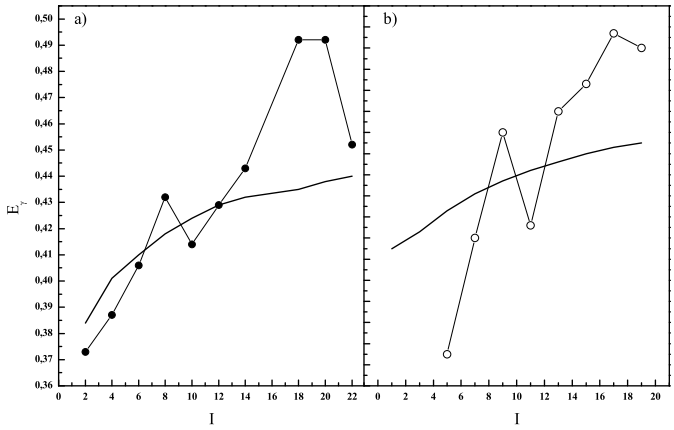

FIGURE 3. Calculated (line) and experimental (solid circles connected by lines) energies of γ transitions between subsequent levels of the ground state band (a) and the first negative parity band (b). Experimental values are taken from [14].

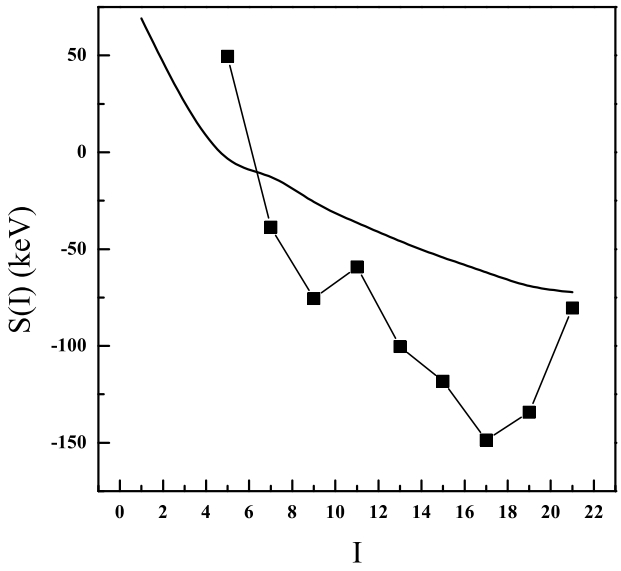

FIGURE 4. Calculated (lines) and experimental (solid squares connected by lines) values of parity splitting (see Eq.(37)). Experimental values are taken from [14].

The model considered above does not provide a mechanism which could be responsible for the experimentally observed behavior of the γ-transition energies. However, it is seen from Fig. 3 that the interval of variation of ω_{vib} with angular momentum observed experimentally and obtained in calculations is not large. The frequencies vary from 185 keV to 240 keV. By taking into account the length of the spectra in both energy and angular momentum, we see that the frequency can be treated with a good accuracy as a constant.

Dependence of the experimental and calculated values of a parity splitting in the ground state and the first negative parity bands, treated as a unified alternating parity

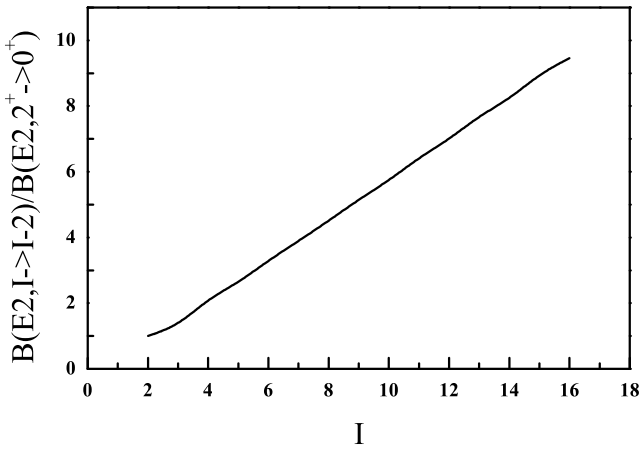

FIGURE 5. Angular momentum dependence of the ration of the reduced transition probabilities $B(E2, I \to (I-2))/B(E2, 2^+ \to 0^+)$ for the quadrupole transitions between the subsequent levels in the ground state band and the first negative parity band.

band, on angular momentum is illustrated in Fig.4. The parity splitting is defined by the expression [14]

$$S(I^-) = E(I^-) - \frac{(I+1)E^+_{(I-1)} + IE^+_{(I+1)}}{2I+1}. \tag{37}$$

It is seen from the figure that for the low angular momenta the parity splitting is positive and becomes negative with angular momentum increase. The possibility for the negative values of the parity splitting is related to the fact that the ground-state band and the first negative parity band are of the vibrational type. In this case the sign of the parity splitting is determined by the difference in the energies characterizing the quadrupole vibrations of the heavy fragment and the rotation of the light fragment around the heavy one. Indeed, in the zero approximation $E(I^-) = \frac{1}{2}\omega(I-1) + \frac{\hbar^2}{2\mu R^2}$, $E(I^+) = \frac{1}{2}\omega I$ and therefore $S(I^-) = \frac{\hbar^2}{2\mu R^2} - \frac{1}{2}\omega\frac{2I}{(2I+1)}$. Thus, for $\frac{\hbar^2}{2\mu R^2} < \frac{1}{2}\omega$, $S(I^-)$ can take negative values. In the case of the rotational bands, the value $S(I)$ must stay positive, achieving a zero value for the ideal unperturbed rotational bands of a nucleus with a stable octupole deformation.

The important feature of the spectra is an appearance at low energy of the second excited negative parity band which contains the states of the even and odd angular momenta. This band has an interesting features. The state with angular momentum I=2 is lower than the state with I=1. With increase of angular momentum the normal level sequence is restored. The reason for such a behavior is related to a significant contribution of the states $\left[|\frac{I+1}{2}\frac{I+1}{2}(I+1)) \times Y_1\right]_{(I+1,M)}$ and $\left[|\frac{I+1}{2}\frac{I+1}{2}(I+1)) \times Y_1\right]_{(I+2,M)}$ into the wave functions for even and odd angular momenta, respectively. In the limit of $\hat{V}_{int}$ is going to zero these two states become degenerate.

It is assumed above that the intrinsic excitations of the heavy cluster are described by the quadrupole harmonic oscillator model. We know that an excitation spectrum generated by this model is characterized by a high degree of a degeneracy. So, it is

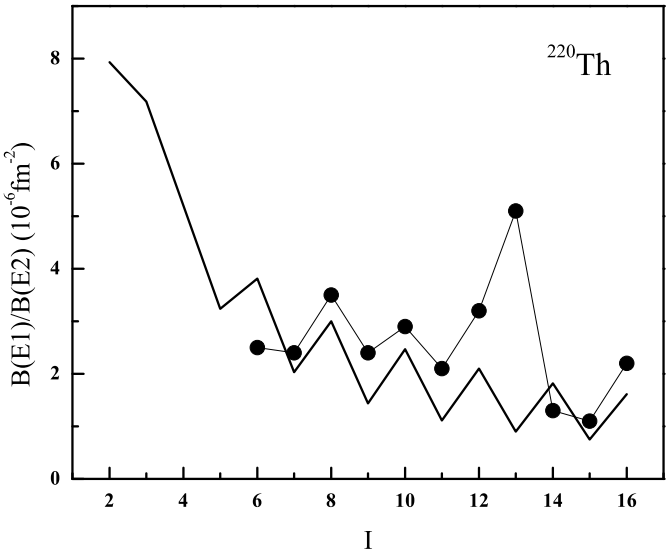

FIGURE 6. $B(E1)/B(E2)$ ratio as a function of the initial angular momentum for transitions in the ground and the first negative parity bands. Experimental values (filled circles) are taken from [14].

interesting to know to what extent the traces of these degeneracies are seen in the spectrum generated by the full Hamiltonian which contains also the interaction term.

First of all, it is interesting at what excitation energies appears the second excited 2^+ state and the first excited 0^+ state which has the same excitation energy as the 4_1^+ state in the case of the quadrupole harmonic oscillator. For ^{220}Th we obtain E$^*(2_2^+)$=1161 keV and E$^*(0_2^+)$=896 keV. For the E$^*(4_1^+)$ we have 717 keV.

Experimentally the excited bands of the positive parity have not been observed in ^{220}Th. There are known 10^+ and 8^+ states with the excitation energies around 2 MeV. However, it is not clear either these states are two-quasiparticle or they belong to the excited rotational bands. Thus, the experimental information on the excitation energies of the 2_2^+ and 0_2^+ states and on their characteristics is very important for the check of the suggested model.

In Fig.5, the values of the ratio $B(E2, I \to I-2)/B(E2, 2^+ \to 0^+)$ are presented as a function of the initial angular momentum. As it should be in the case of harmonic quadrupole oscillations of the heavy fragment the values of $B(E2)$ increase linearly with I. They does not show any changes in the behavior for transitions between the members of the ground-state band and the first negative parity band since the underlying quadrupole constituents in both bands are the same. Thus, the experimentally observed staggering of the $BE1/BE2$ ratios can be attributed to the staggering of the $B(E1)$ values (see Fig. 6).

Such a staggering behavior of $B(E1)$ can be qualitatively explained analyzing the equation (36). We can see that the reduced transition probability B(E1) for the transition from the state I of the ground state band to the state (I-1) of the first excited negative parity band consist of two contributions, since both dipole transitions are allowed (see Eqs.(19,22)): from the component $\left[|\frac{I}{2}\frac{I}{2}(I)) \times Y_0\right]_{(IM)}$ to $\left[|\frac{I}{2}\frac{I}{2}(I)) \times Y_1\right]_{(I-1,M)}$ and from

the component $\left[|\frac{I-2}{2}\frac{I-2}{2}(I-2))\times Y_2\right]_{(IM)}$ to $\left[|\frac{I-2}{2}\frac{I-2}{2}(I-2))\times Y_1\right]_{(I-1,M)}$. In the opposite case of transition from the states of the negative parity band to the states of the positive parity belonging to the ground state band, we have only one allowed transition, namely, from the component $\left[|\frac{I}{2}\frac{I}{2}(I))\times Y_1\right]_{(I+1,M)}$ to the component $\left[|\frac{I}{2}\frac{I}{2}(I))\times Y_0\right]_{(I,M)}$. The transition from $\left[|\frac{I+2}{2}\frac{I+2}{2}(I+2))\times Y_1\right]_{(I+1,M)}$ to $\left[|\frac{I-2}{2}\frac{I-2}{2}(I-2))\times Y_2\right]_{(I,M)}$ is forbidden because the dipole operator does not change a number of the quadrupole phonons.

The $B(E1)/B(E2)$ ratio as a function of an initial angular momentum is presented in Fig.6. Calculated ratios for the odd initial angular momentum (i.e. for transitions from the states of the negative parity) lie systematically lower than the ratios for the even initial angular momentum (transitions from the state of the ground state band). This is in agreement with the experimental data with the exception of two data points at 13^- and 14^+ . As it is mentioned in [14] the large value of $B(E1)/B(E2)$ ratio at 13^- can be attributed to the loss of $E2$ strength in the backbending. The rather small $B(E1)/B(E2)$ value for the 14^+ attributed to the spread of $E1$ strength due to the presence of two 13^- final states.

CONCLUSION

We have suggested a cluster interpretation of the properties of the multiple negative parity bands in ^{220}Th. The collective motion related to the cluster degree of freedom leads to the admixture of the very asymmetric cluster configurations to the intrinsic nucleus wave function. To take into account the reflection asymmetric modes with nonzero values of K, the harmonic quadrupole oscillations of the heavy cluster is considered. The resulting energy spectrum consists of the ground state band and several negative parity bands which exhibit nearly equidistant behavior. The angular momentum dependence of the parity splitting is described. The possibility for the negative values of the parity splitting is related in the model to the interplay between the quadrupole vibrations of the heavy fragment and the rotational motion of the light fragment. We describe the observed staggering behavior of the $B(E1)/B(E2)$-rations as a function of the angular momentum. The $BE(1)$ transitions from the state of the negative parity to the state of the positive parity is hindered, in this case in a contrast to the transitions from the positive to the negative parity state the $E1$ transition operator relates only a part of the components of the wave functions of the bands. The results of calculations are in overall agreement with the experimental data. This work is a further development of the previously developed approaches [7, 10, 11].

REFERENCES

1. P. Butler and W. Nazarewicz, *Rev. Mod. Phys.* **68**, 349 (1996).
2. F. Iachello and A.D. Jackson, *Phys. Lett.* **B108**, 151 (1982).
3. W.D.M. Rae, *Int. J.Mod. Phys.* **A3**, 1343 (1988).
4. M.Freer, A.C. Merchant, *J.Phys.* **G23**, 261 (1997).
5. W. Nazarewicz, J.X. Saladin et al., *Phys. Lett.* **B322**, 304 (1994).
6. S. Aberg, L.-O. Jonsson, *Z. Phys.* **A349**, 205 (1994).

7. T.M. Shneidman et al. *Nucl. Phys.* **A671**, 119 (2000).
8. Ch. Briancon, and I.N. Mikhailov, in *Proc. Int. Conf. on Nucl. Structure, Reactions and Symmetries*, edited by R. A. Meyer and V. Paar, World Scientific, Singapore, 1986, v.1, p.131.
9. S. Frauendorf, *Phys. Rev.* **C77**, 021304(R) (2008).
10. T.M.Shneidman, G.G.Adamian, N.V.Antonenko, R.V.Jolos, *Phys.Rev.* **C74**, 034316 (2006).
11. T.M.Shneidman, G.G.Adamian, N.V.Antonenko, R.V.Jolos, W.Scheid, *Phys.Rev.* **C67**, 014313 (2003).
12. G.G.Adamian, N.V.Antonenko, R.V.Jolos, Yu.V.Palchikov, W.Scheid, T.M.Shneidman, *Phys.Rev.* **C69**, 054310 (2004).
13. G.G.Adamian, N.V.Antonenko, R.V.Jolos, Yu.V.Palchikov, W.Scheid,*Phys.Rev.* **C67**, 054303 (2003).
14. W. Reviol et al., *Phys. Rev.* **C74**, 044305 (2006).
15. W. Nazarewicz, G.A. Leander, and J. Dudek, *Nucl. Phys.* **A467**, 437 (1987).
16. T. Otsuka, and M. Sugita, *Phys. Lett.* **B209**, 140 (1988).
17. G.G. Adamian, N.V. Antonenko, R.V. Jolos, S.P. Ivanova and O.I. Melnikova, *Int. J. Mod. Phys.* **E5**, 191 (1996).
18. W.Bonin et al., *Z. Phys.* **A322**, 59 (1985).
19. N. Schulz et al., *Phys. Rev. Lett.* **63**, 2645 (1989).